Production of active coal from pyrolyzed wood wastes by alkaline activation of KOH

Oleg Kuzmin[1], Julia Tamarkina[2], Tetiana Shendrik[2], Valentyna Zubkova[3], Olga Koval[1], Tetiana Roman[1]

1 – National University of Food Technologies, Kyiv, Ukraine
2 – L.M. Litvinenko Institute of Physical–Organic Chemistry and Coal Chemistry of the National Academy of Science of Ukraine, Kyiv, Ukraine
3 – Jan Kochanowski University in Kielce, Kielce, Poland

Keywords:

Pyrolysis
Wood
Wastes
Alkaline activation
Active coal
Nanopores

Article history:

Received 6.06.2017
Received in revised form 30.08.2017
Accepted 05.09.2017

Corresponding author:

Oleg Kuzmin
E-mail:
kuzmin_ovl@
nuft.edu.ua

DOI: 10.24263/2304-974X-2017-6-3-5

Abstract

Introduction. The purpose of this publication is to evaluate an alternative renewable raw materials obtained from the food industry wastes (pyrolyzed wood wastes – PWW) as precursors for production of active coal (AC) used in a process of water purification in alcoholic beverages' production.

Materials and methods. PWW of meat processing industry. PWW will be used as a raw material for a production of AC. Chemical activation of PWW by alkaline activation of *KOH*. Method of adsorption–desorption of nitrogen to determine a porous structure at 77 K; mesopores' distribution by size and by mesopores' volume – *BJH*-method; micropores' division by size – *QSDFT*-method; volume of micropores – Dubinin-Radushkevich method; subnanopores' volume – *QSDFT*–method.

Results and discussion. The microporous structure has the following characteristics: pores' diameters are in the range of D_{mi}=0,61–2,5 nm, most represented pores' diameters are 0,61; 1,19; 1,54 nm; volume of micropores – V_{mi}=0,11–0,30 cm^3/g; pores' surface area – S_{mi}=407–852 m^2/g; pores' differential volume – dV_{mi}/dD=(0,023–1,400)·10^{-2} cm^3/g; pores' differential area – dS_{mi}/dD=(0,18–45,60) m^2/g. There are 70,31% of micropores in a total pores' volume. Dominant contribution of micropores into specific surface of the pores shows a proportional dependence between pores' volume and surface area of pores. It is also confirmed by the linear dependence between the pores' differential volume and the differential area. The smallest pores – subnanopores with $D\leq1$ nm were defined at the micropores structure. Subnapores' diameters are in the range of D_{1nm}=0,61–1,00 nm. Subnanopores' volume varies in the range of V_{1nm}=0,11–0,25 cm^3/g. Pores' surface area is S_{1nm}=407–783 m^2/g; pores' differential volume: dV_{1nm}/dD=(11,3–140,0)·10^{-4} cm^3/g; differential area is dS_{1nm}/dD=(2,33–45,60) m^2/g. The subnanopores' portion at the micropores' volume is 84,12%. The share of subnanopores' at the total pores' volume is 59,15%. It can be argued that the alkaline activation of *KOH* leads to a development of subnanopores in the porous structure of the adsorbent. The cited data shows that the proposed method allows to obtain AC with an output ratio of 70,4%. The obtained AC has a developed specific surface of S_{BET}=777 m^2/g and porosity. Total pores' volume is V_{Σ}=0,421 cm^3/g.

Conclusion.. An energy–saving method is proposed for the production of high porous AC from the secondary «renewable» resources – PWW. It is advised to use it in alcoholic beverages production.

Introduction

A search for economically feasible ways of obtaining cheap sorbent materials in a purification of contaminated environment remains an urgent problem for all the countries around the world. Carbon adsorbents occupy a significant place among such materials. This kind of raw material has a gigantic range of precursors (natural coal, peat, wood, carbonaceous wastes of various origins, etc.) [1–12]. Therefore, there is an urgent need to obtain AC from an alternative material. The search for these materials could involve existing technologies of food industry. Wastes from these industries can be used to produce the adsorbents [4-8, 11-26].

There two ways of getting AC that are known today: chemical [1, 4–6, 10–13, 15, 16, 19, 21–23, 26–28] and physical activation [1, 10, 15, 17, 21]. Benefits of chemical activation are one-step process; low activation temperature; short activation time; large yield; high surface; well-developed controlled microporosity [28]. Chemical activation involves usage of activating agent ($ZnCl_2$ [4], H_3PO_4 [9, 11, 12, 16, 23, 26], *NaOH* [28], *KOH* [27, 28], et al.), entered by impregnation, followed by carbonization of raw materials in the atmosphere of inert gases and activation [1].

There are many ways of receiving AC (Kumar, Jena, 2017; Yorgun, Yildiz, 2015; Kucherenko et al, 2010; Lillo-Rodenas, 2003) [4, 11, 27, 28], (Pat. 61059 Ukraine): grinding carbon-containing material with $(1–2)\cdot10^{-3}$ m, mixing it with *KOH* in solid form in a weight ratio 1:1, carbonizing and activating at heatstroke mode, cleaning with water and drying. This method (Pat. 61059 Ukraine) has its disadvantages: raw materials grinding has a high energy consumption; the small size of raw materials' fractions – it became charcoaled after carbonization and activation and evaporates with a gaseous components; high temperature carbonization and activation of AC; activation in a heatstroke mode causes tearing of the structure and reduction of AC shares; low rate of AC release.

The most promising raw material for AC is PWW. PWW is formed by pyrolysis of wood chips (Kuzmin, Shendrik, 2016) [10]. In a proposed method grinding materials are not required as AC wood chips' size is $l\times b\times h=(6\times12\times3)\cdot10^{-3}$ m; AC fractional increases up to $3{,}6\cdot10^{-3}>d\geq1{,}0\cdot10^{-3}$ m; temperature reduction of charcoal's carbonization and activation within T=773–973 K; absence of activation heat stroke due to carbonization at non-isothermal heating and isothermal heating at activation; yield increases of AC ratio.

KOH is one of the promising activating agents (Kucherenko V.A. et al, 2010; M.A. Lillo-Ródenas et al, 2007) [27, 28]. It is added to the brown coal. It can withstand up to full impregnation, allowing alkali to interact with organic and mineral components, with the formation of water-soluble substances washed with AC.

Thus, the use of *KOH* allows to receive AC with a formed pores' space. Variation of mass part (MP) of activating agent in relation to PWW can affect the surface pores' factor, yield ratio of AC and volume of wastewater [29-37].

A blend of raw material/agent during carbonization and activation undergoing non-isothermal heating up to an activation temperature during the subsequent isothermal aging. At the same time low molecular parts of thermal distraction of organic matter of PWW and products of PWW's chemical reactions with alkali are formatted in a PWW's volume. It's outflow from the PWW's volume creates a spatial framework within PWW. It leads to a formation of micropores and subnanopor and, consequently, increases the pores' specific surface area and total volume. This improves adsorption characteristics of AC (Shendrik et al, 2003; Kucherenko et al, 2010; Zubkova, 2011) [27, 29, 30]. AC's fractional composition is determined by MP's residue on sieves with holes with a diameter of 3,6 mm, 1,0 mm and on the pallet itself.

It has been shown that PWW can be an alternative carbon-containing raw material for AC

production (Kuzmin, Shendrik, 2016) [10]. The aim of this work is to evaluat an alternative renewable raw materials from the food industry wastes (pyrolyzed wood wastes – PWW) as precursors for production of active coal (AC) which can be used for water purification in alcoholic beverages' production.

Materials and methods

Conditions for AC production are presented at Table 1.

Table 1

Terms of AC

Symbol	Characteristic	Experimental data	Rationed data
T_1	Drying temperature in the open air, K	295	293–298
W_1	Relative humidity,%	74	67–82
v_1	Air traffic speed, m/s	1,5	1–2
τ_1	PWW's outdoor drying time, s	$336 \cdot 60^2$	$(336–504) \cdot 60^2$
T_2	Drying temperature in the drying cabinet, K	373	373–383
W_2	MP of moisture of PWW,%	6,58	4–8
	MP of *KOH* in aqueous solution,%	50	30–70
	Mass ratio (MR) of PWW/alkali, kg/kg	1:1	1:0,5–1:1
τ_2	Time withstand of PWW with alkali, s	$24 \cdot 60^2$	$(18–24) \cdot 60^2$
T_3	PWW alkali holding temperature, K	294	291–295
T_4	Drying temperature, K	381	373–383
W_3	MP of moisture of PWW,%	6,78	4–8
Q_1	Volumetric flow of argon, m^3/s	$5,6 \cdot 10^{-7}$	$\leq 5,6 \cdot 10^{-7}$
	Non-isothermal heating, deg./s	0,07	≤0,07
	MP of sulfuric acid,%	96	96
T_5	Activation temperature, K	1073	873–1073
τ_3	Time of activation, s	$1 \cdot 60^2$	$1 \cdot 60^2$
	Non-isothermal cooling, deg./s	0,1	≤0,1
T_6	Final temperature after cooling of AC, K	323	≤323
τ_4	Time cleaning of AC from activating agent, s	600	300–600
T_7	Drying temperature in the drying cabinet, K	378	373–383
W_4	MP moisture AC,%	5,84	4–8
Y_1	AC yield ratio,%	70,4	70–80
	MP of remnant of AC (%) in the sieve with holes, m:		
	$d \geq 3,6 \cdot 10^{-3}$	0,2	MP≤2,5
	$3,6 \cdot 10^{-3} > d \geq 1,0 \cdot 10^{-3}$	87,6	MP≥95,5
	$d < 1,0 \cdot 10^{-3}$	12,2	MP≤2,0

Obtained PWW is dried in the open air (T_1=293–298 K; W_1=67–82%; v_1=1–2 m/s) during $\tau_1=(336–504) \cdot 60^2$ s, followed by more drying at T_2=373–383 K up to air–dry state with humidity of W_2=4–8%.

KOH (MP *KOH* in aqueous solution – 30–70%) used as an activating agent for impregnating

of PWW/alkali in MR 1:0,5–1:1. The received mixture withstands for τ_2=(18–24)·60^2 s at T_3=291–295 K and PWW dried to receive a constant weight of MP moisture W_3=4–8% at T_4=373–383 K. Activation carried out in a stream of argon with a volumetric flow of $Q_1 \leq 5{,}6 \cdot 10^{-7}$ m^3/s with drying bubbling after 96% in sulfuric acid under non-isothermal heating at 0,07 deg./s up to activation temperature T_5=873–1073 K and isothermal aging for τ_3=1·60^2 s at the temperature activation and non-isothermal cooling at 0,1 deg./s in a stream of argon upto a temperature T_6 = 323K.

The received AC cleaned from activating agent with a usage of water for τ_4=300–600 s and dried at a temperature T_7=373–383 K up to a level of humidity W_4=4–8% with the yield of AC Y_1=70–80%, followed by fractioning with the help of MP residue on sieves with holes: $d \geq 3{,}6 \cdot 10^{-3}$ m – MP≤2,5%; $3{,}6 \cdot 10^{-3} > d \geq 1{,}0 \cdot 10^{-3}$ m – MP≥95,5%; $d < 1{,}0 \cdot 10^{-3}$ m – MP≤2,0% with the following selection of working faction on a sieve with holes $3{,}6 \cdot 10^{-3} > d \geq 1{,}0 \cdot 10^{-3}$ [9].

Figure 1 shows the stages of AC production; Figure 2 – general scheme of AC obtaining as per experimental data at Table 1.

Figure 1. Stages of receiving AC:
a – technological chips of oak large (6x12x3)·10^{-3} m; *b* – PWW with MP moisture W=43,01%; *c* – PWW after drying of moisture MP W=6,58%; *d* – AC to fractionation; *e* – AC after fractionation of $d \geq 3{,}6 \cdot 10^{-3}$ m; *f* – AC after fractionation of $3{,}6 \cdot 10^{-3} > d \geq 1{,}0 \cdot 10^{-3}$ m; *g* – AC after fractionation of $d < 1{,}0 \cdot 10^{-3}$ m

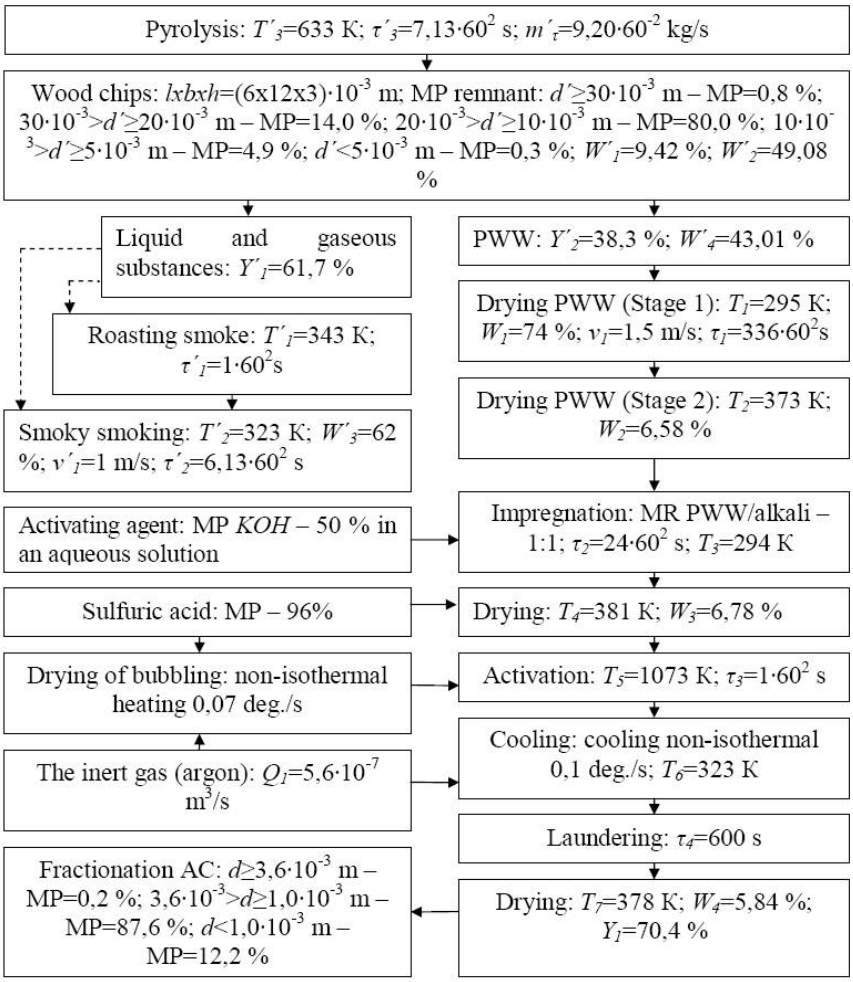

Figure 2. The general scheme of AC production as per experimental data

PWW dried for τ_1=336·60^2 s outdoors (T_1=295 K; W_1=74%; v_1=1,5 m/s), followed by drying at the drying cabinet at T_2=373 K to air-dry state with MP moisture – W_2=6,58%. Potassium hydroxide with MP *KOH* – 50% in am aqueous solution, injected by impregnation of PWW – *KOH* and kept for τ_2=24·60^2 s at temperature T_3=294 K, dried up to a moisture obtained at MP PWW W_3=6,78% at T_4=381 K. The volume of solution has been chosen to create MR PWW/alkali – 1:1 kg/kg. Activation was performed in a vertical cylindrical tubular reactor made of steel, with thickness of 3 mm, diameter of cylinder – 0,15 m, height – 0,3 m.

The reactor was purged with argon volumetric flow of Q_1=5,6·10^{-7} m^3/s, drained bubbling through concentrated sulfuric acid (96%). The heating of reactor's furnace has been switched on after 0,17·60^2 s after the start of argon input. The temperature mode of process included a period of non-isothermal heating (0,07 deg./s) up to an activation temperature, isothermal holding at this temperature for τ_3=1·60^2 s and rapid cooling in a

stream of argon cooled at non-isothermal 0,1 deg./s to T_6=323 K. Activation temperature was T_5=1073 K when activated via *KOH*.

Samples of AC activating agent washed with distilled water for τ_4=600 s and dried at T_7=378 K to humidity W_4=5,84% of the yield of AC Y_1=70,4%. Fractionation AC remnant of MP conducted on sieves with holes: $d \geq 3{,}6 \cdot 10^{-3}$ – MP=0,2%; $3{,}6 \cdot 10^{-3} > d \geq 1{,}0 \cdot 10^{-3}$ – MP=87,6%; $d < 1{,}0 \cdot 10^{-3}$ (pallet) – MP=12,2% with the following collection of working fractions on sieves of 3,6 mm and 1,00 mm MP – 87,8%.

Results and discussions

Characteristics of porous structure was determined on a basis of isotherms of an adsorption-desorption of nitrogen at T=77 K in the range of relative pressure P/P_0=0,00–1,00 (device Quantachrome Autosorb 6B) (Figure 3).

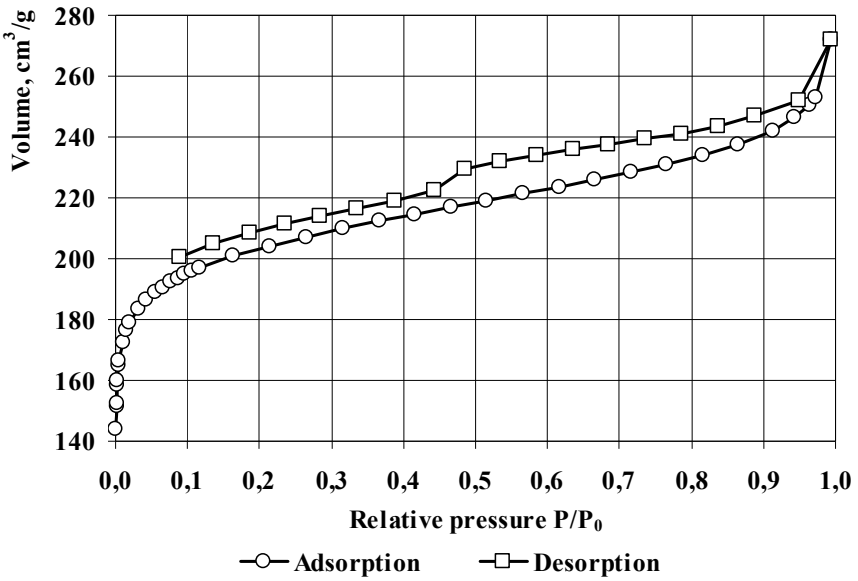

Figure 3. Isotherms of an adsorption-desorption of nitrogen at AC at T=77 K

The obtained isotherms of type II – according to Brunauer S. et al, 1938 [31] classification, per multimolecular adsorption. Sorption hysteresis loop approaching the point of relative pressure P/P_0=0,4, indicating a predominance of micropores of meso- and macropores.

Figures 4–7 shows the distribution of micropores (*QSDFT*–method), the size of the sample and the corresponding volumes accumulated in these pores.

The microporous structure has the following characteristics (Figure 4–5): pore diameters are in the range of D_{mi}=0,61–2,5 nm, mostly represented by pores with a diameter of 0,61; 1,19; 1,54 nm; volume of micropores – V_{mi}=0,11–0,30 cm^3/g; pores' surface area – S_{mi}=407–852 m^2/g; pores' differential volume dV_{mi}/dD=(0,023–1,400)$\cdot 10^{-2}$ cm^3/g; pores' differential area dS_{mi}/dD=(0,18–45,60) m^2/g; micropores are about 70,31% of the total pore volume.

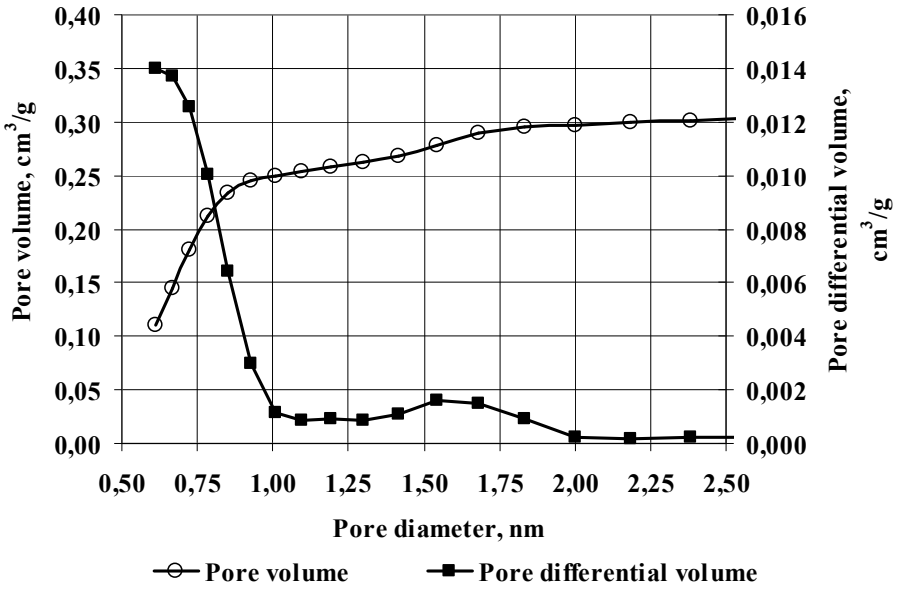

Figure 4. Distribution of micropores by size of AC sample – (dependence of pores' volume and pores' differential volume on pores' diameter) by *QSDFT*–method

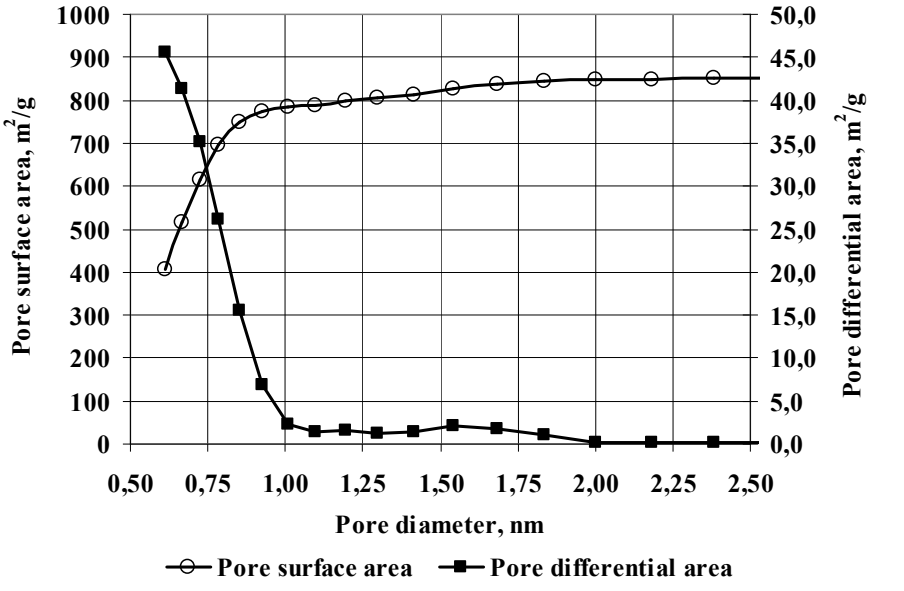

Figure 5. Distribution of micropores by size of AC sample – (dependence of surface area and pores' differential surface area on pores' diameter) by *QSDFT*–method

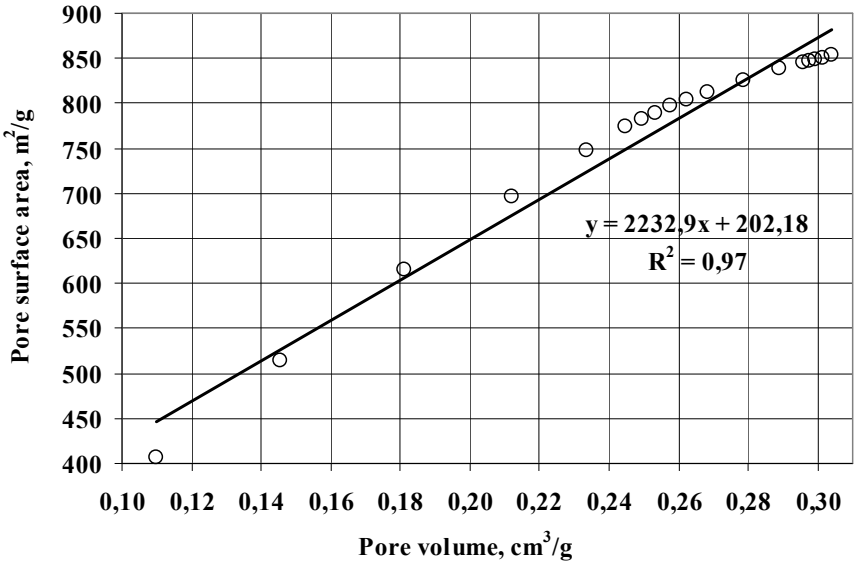

Figure 6. Distribution of micropores by size of AC sample – (dependence of pores' volume on pores' surface area) by *QSDFT*–method

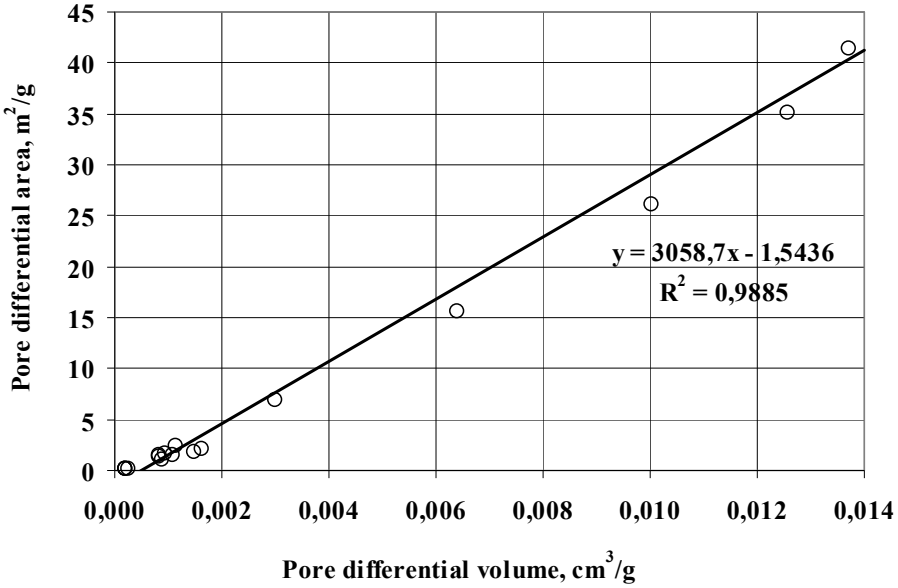

Figure 7. Distribution of micropores by size of AC sample – (dependence of pores' differential volume on pores' differential surface area) by *QSDFT*–method

According to distribution of micropores by size, two areas of values can be distinguished: a dynamic range (D_{mi}=0,5–2,0 nm) of values with several maxima; a stationary range of values (D_{mi}=2,0–2,5 nm). The main differences are fixed at the dynamic range of values (D_{mi}=0,5–2,0 nm). We can observe three maximum values: at ~ 0,6 nm, weakly expressed at ~ 1,2 nm, maximum at ~ 1,5 nm. The differential pore volume is in the range of dV_{mi}/dD=(1,9–2,1)·10^{-4} cm^3/g at the static range of values D_{mi}=2,0–2,5 nm. The differential area is in the range of dS_{mi}/dD=(0,18–0,20) m^2/g.

The dominant contribution of micropores in the specific surface of the pores shows a proportional relationship between the pores volume and the surface area of pores. This is also confirmed by the linear dependence between the pores' differential volume and the pores' differential area (Figure 6–7).

The subnanopores with $D \leq 1$ nm – the smallest pores were considered in the micropores' structure (Figure 4–5): pores' diameters are in the range of D_{1nm}=0,61–1,00 nm; subnanopore's volume varies in the range of V_{1nm}=0,11–0,25 cm^3/g; pores' surface area: S_{1nm}=407–783 m^2/g; pores'differential volume: dV_{1nm}/dD=(11,3–140,0)·10^{-4} cm^3/g; pores' differential area: dS_{1nm}/dD=(2,33–45,60) m^2/g. The subnanopore's portion in the micropores volume is 84,1%. The share of subnanpore's in the total pores' volume is 59,2%. It can be argued that the alkaline activation of *KOH* leads to the development of a subnanopore's in the porous structure of the adsorbent.

Figures 8–13 show the distribution of mesopores (*BJH*–method) by size in the sample and the corresponding volumes accumulated in these pores.

In Figure 8, the curve of the pores' size set with its size increasing smoothly, not reaching the plateau, indicating the presence of mesopores with a wide distribution in size.

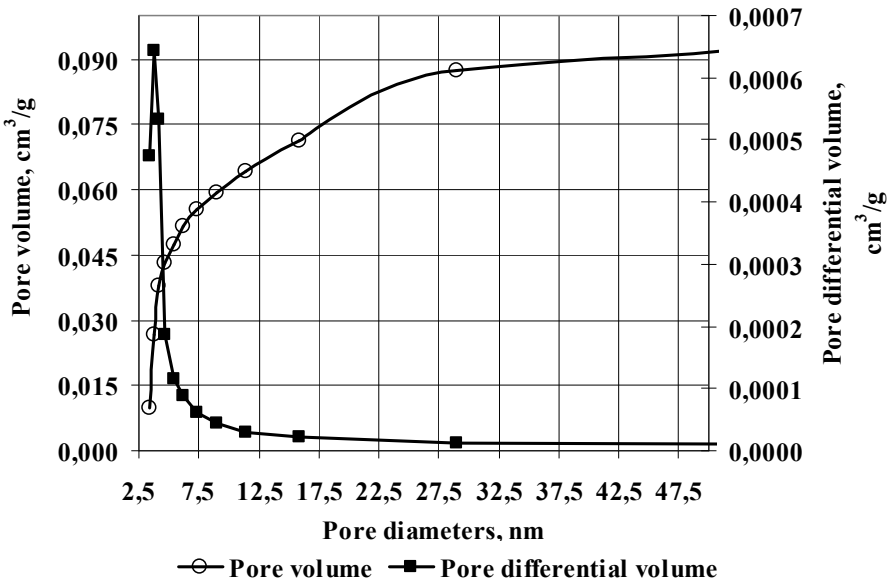

Figure 8. Distribution of mesopores by size of AC sample – (dependence of pores' volume and pores' differential volume on pores' diameter) by *BJH*–method

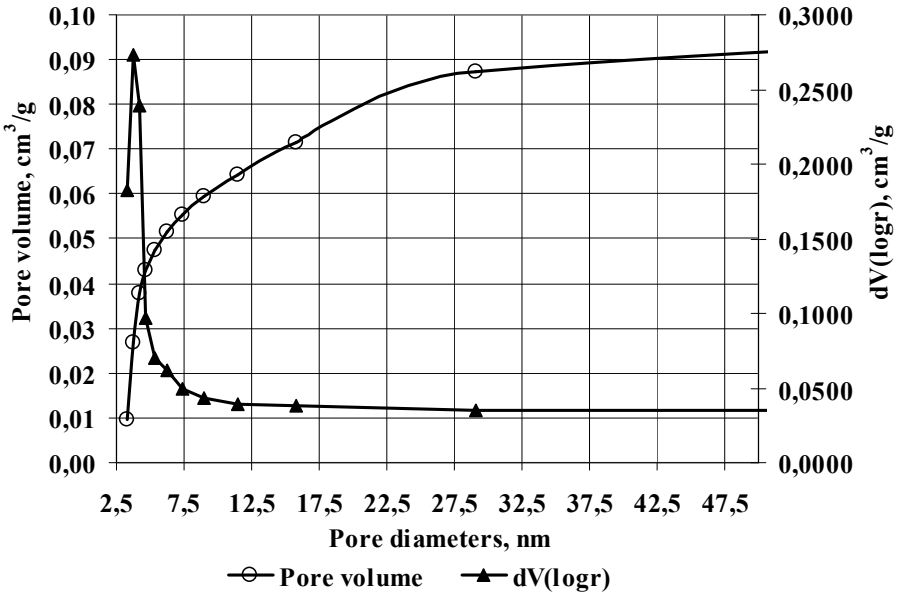

Figure 9. Distribution of mesopores by size of AC sample – (dependence of pores' volume and pores' *dV(logr)* on s' diameter) by *BJH*–method

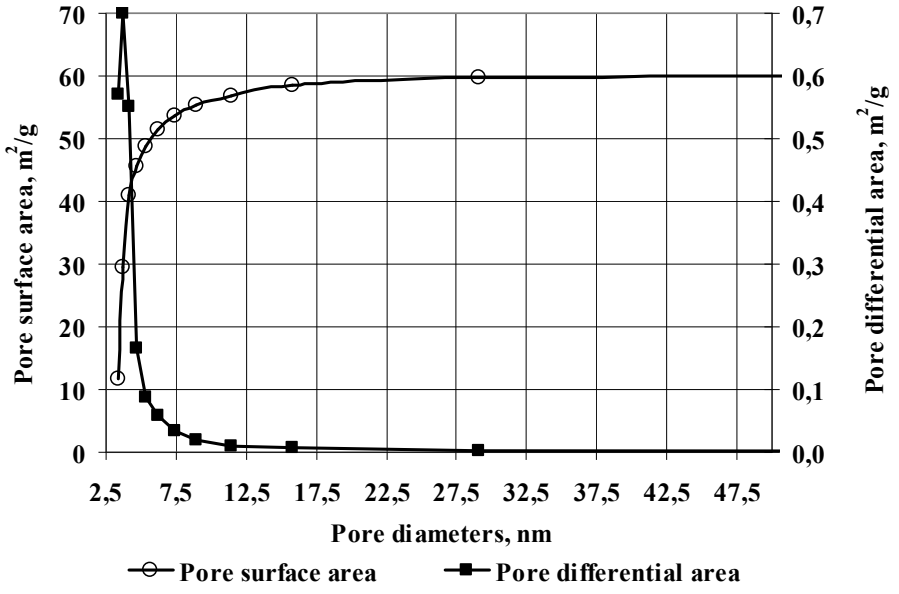

Figure 10. Distribution of mesopores by size of AC sample – (dependence of pores' surface area and pores' differential surface area on pores' diameter) by *BJH*–method

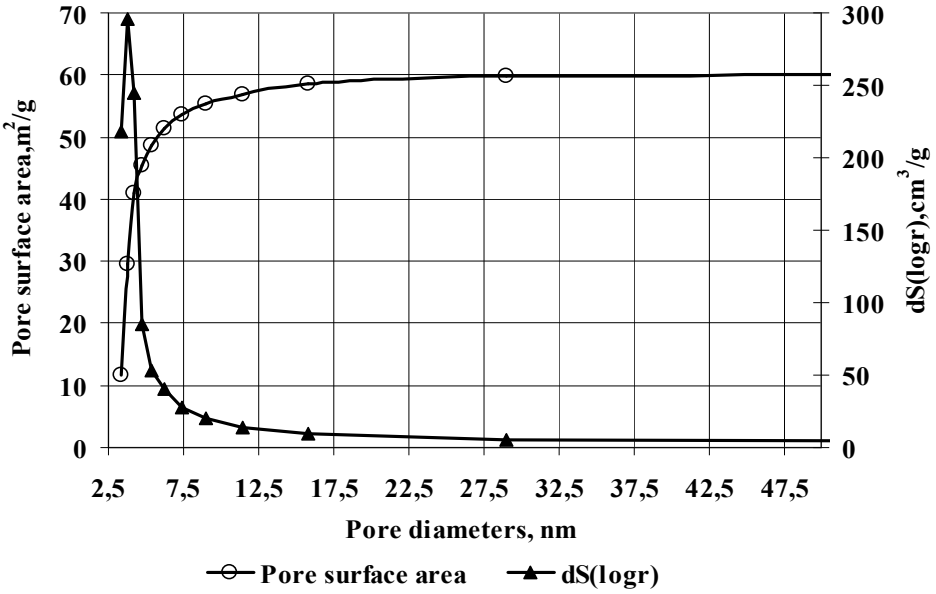

Figure 11. Distribution mesopores the size of AC sample – (dependence of pores' surface area and pores' *dS(logr)* on pores' diameter) by the *BJH*–method

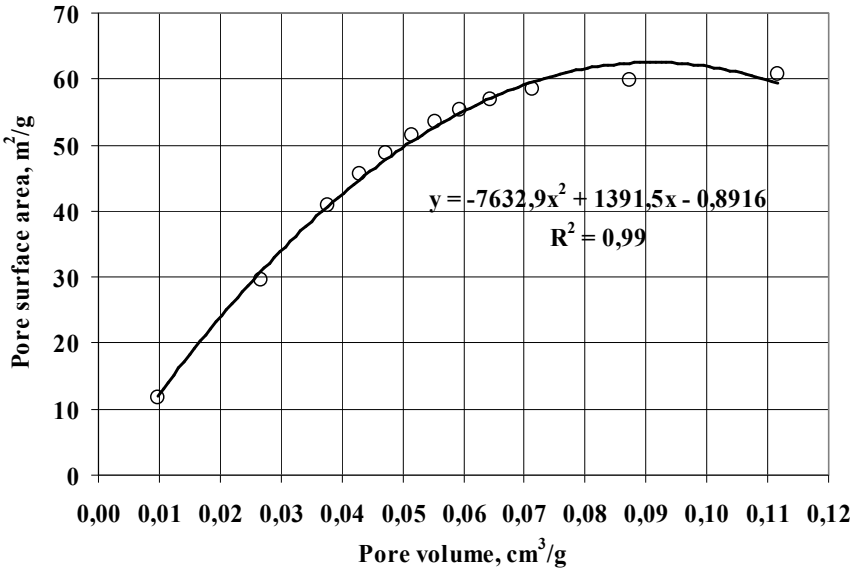

Figure 12. Distribution of mesopores by size of AC sample – (dependence of pores' surface area on pores' volume) by the *BJH*–method

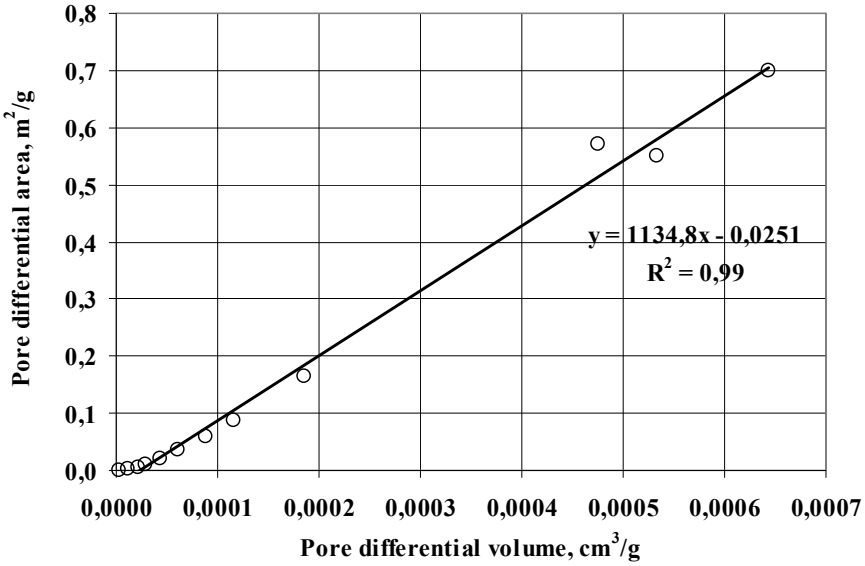

Figure 13. Distribution of mesopores by size of AC sample – (dependence of pores' differential area on pores' differential volume) by the *BJH*–method

Mesoporous structure has the following characteristics: pores' diameters are in the range of D_{me}=3,3–50,0 nm, most represented pores with a diameter of 3,73 nm; mesopore volume varies in the range of V_{me}=0,010–0,091 cm^3/g; pores' surface area – S_{me}=11,7–60,0 m^2/g; pores' differential volume dV_{me}/dD=(0,02–4,75)·10^{-4} cm^3/g; pores' differential area dS_{me}/dD=(0,002–0,570) m^2/g; fraction of mesopores in the total pores' volume is 2,14–21,6% (Figure 8–13).

Curves of pores' differential volume and pores' differential surface area at the interval of D=15,8–50,0 nm are in the static area. Maximum location of pores with a smallest diameter is observed at the pores' differential volume dV_{me}/dD=6,43·10^{-4} cm^3/g at the point of 3,73 nm within D=2,5–15,8 nm. The biggest number of mesopores are located at the range of D=2,5–15,8 nm.

The terms of AC and its characteristics are shown at the Table 2. The following characteristics of AC were measured: Y – yield (%); S_{BET} – specific surface area; V_{Σ} – pores' total volume; V_{ma} – macropores' volume; V_{me} – mesopores' volume; V_{mi} – micropores' volume; V_{1nm} – subnanopores' volume; A_{Phenol} – sorption capacity toward phenol; A_{Pb} – sorption capacity toward Plumbum; A_{MB} – sorption capacity toward methylene blue.

Comparison of distribution of porous space according to (Pat. 61059 Ukraine) to the experimental data is presented at the figure 14.

A method that allows the production of AC from PWW, generated after the process of food products' smoking has been proposed. Moreover, PWW is subsequently heated non-isothermally and chemically activated in the presence of *KOH*. As a result, AC is produced with a high yield of 70–80%, developed specific surface, porous space and a high sorption capacity. The results of AC production can be adapted for the technology of alcoholic beverages' production at the expense of 1,0–3,6 mm particles' fractional composition.

Table 2

Terms of AC and its characteristics

Characteristic	Method of AC production (Pat. 61059 Ukraine)		Method of AC experimental production	
Type of raw material	Lignite (brown coal)		PWW	
Activation temperature, K	1073		1073	
Activating agent	*KOH*		*KOH*	
State of the activating agent	solid		solution 50%	
MR raw/agent, kg/kg	1:0,5		1:1	
Y,%	39,0		70,4	
S_{BET}, m^2/g	890		777	
V_{Σ}, cm^3/g	0,580	100%	0,421	100%
V_{ma}, cm^3/g	0,010	1,73%	0,034	8,08%
V_{me}, cm^3/g	0,250	43,10%	0,091	21,61%
V_{mi}, cm^3/g	0,320	55,17%	0,296	70,31%
V_{1nm}, cm^3/g	0,230	39,66%	0,249	59,15%
A_{Phenol}, mg/g	120		200	
A_{Pb}, mmol/g	–		0,7	
A_{MB}, mg/g	92		150	

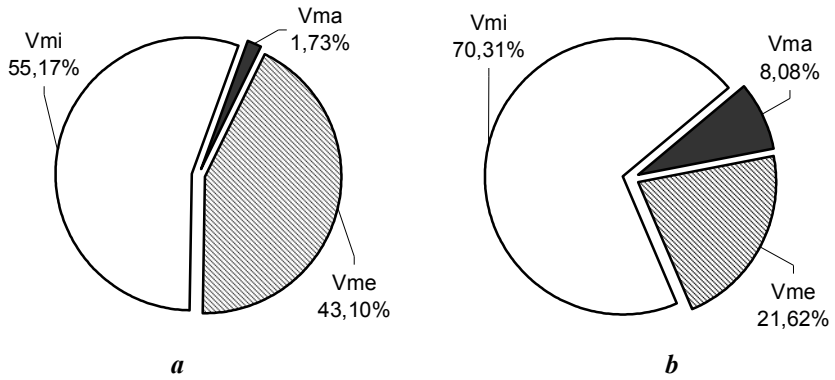

Figure 14. Distribution of pores in AC:
a – according to Pat. 61059 Ukraine; *b* – according to experimental data.

The attention is drawn to the volume of pores' with $D \leq 1$ nm. It accounts to 59,15% of the total pores' volume in AC. The obtained data allows us to hope that the studied raw materials can be used for the purification of water-alcohol mixtures.

Conclusions

The data show that the proposed method allows to obtain AC with a high yield of 70,4% compared to the method of obtaining AC from lignite (Pat. 61059 Ukraine) – 39,0%. Experimentally received AC has a lower specific surface S_{BET}=777 m^2/g with respect to AC (Pat. 61059 Ukraine) S_{BET}=890 m^2/g and pores' space: total pores' volume V_{Σ}=0,421 cm^3/g to V_{Σ}=0,580 m^3/g. Nevertheless, the ratio of micropores in the experimental sample (70,31%), increased in relation to the prototype (55,17%), and the ratio of subnanopores in the experimental sample (59,15%), increased in relation to the prototype (39,66%). The ratio of macropores in the experimental sample (8,08%), increased in relation to the prototype (1,73%). At the same time the ratio of mesopores in the experimental sample (21,61%) reduced relatively to the prototype (43,10%).

It can be concluded that the proposed method of AC production from PWW, produced of smoked foods, with further carbonization at non-isothermal heating and activation at temperature of 873–1073 K in the presence of *KOH*, leads to sorbents with a high yield of 70–80% and fractional composition of particle size of 1,0–3,6 mm (~ 90%). An energy-saving method is proposed for a production of cheap AC from secondary «renewable» resources – PWW. These AC can be examined for water purification in alcoholic beverages' production.

References

1. Marsh H., Rodriguez-Reinoso F. (2006), *Activated carbon*, Amsterdam, Elsevier.
2. J. Rivera-Utrilla, M. Sánchez-Polo, V. Gómez-Serrano, P.M. Álvarez, M.C.M. Alvim-Ferraz, J.M. Dias (2011), Activated carbon modifications to enhance its water treatment applications. An overview, *J. Hazardous Materials*, 187(1–3), pp. 1–23.
3. R.C. Bansal, M. Goyal (2005), *Activated carbon adsorption*, Boca Raton: Taylor&Francis Group.
4. Arvind Kumar, Hara Mohan Jena (2017), Adsorption of Cr(VI) from aqueous phase by high surface area activated carbon prepared by chemical activation with $ZnCl_2$, *Process Safety and Environmental Protection*, 109, pp. 63–71.
5. Aghdas Heidari, Habibollah Younesi, Alimorad Rashidi, AliAsghar Ghoreyshi (2014), Adsorptive removal of CO_2 on highly microporous activated carbons prepared from Eucalyptus camaldulensis wood: Effect of chemical activation, *Journal of the Taiwan Institute of Chemical Engineers*, 45 (2), pp. 579–588.
6. Metin Acikyildiz, Ahmet Gurses, Semra Karaca (2014), Preparation and characterization of activated carbon from plant wastes with chemical activation, *Microporous and Mesoporous Materials*, 198, pp. 45–49.
7. Mohammad Amir Firdaus Mazlan, Yoshimitsu Uemura, Suzana Yusup, Fathelrahman Elhassan, Azhar Uddin, Ai Hiwada, Mitsutaka Demiya (2016), Activated Carbon from Rubber Wood Sawdust by Carbon Dioxide Activation, *Procedia Engineering*, 148, pp. 530–537.
8. B. Ruiz, N. Ferrera-Lorenzo, E. Fuente (2017), Valorisation of lignocellulosic wastes from the candied chestnut industry. Sustainable activated carbons for environmental applications, *Journal of Environmental Chemical Engineering*, 5 (2), pp. 1504–1515.
9. Kuzmin O., Shendrik T., Zubkova V. (2017), Substantiation of the conditions of obtaining porous carbon materials from pyrolyzed wood wastes by chemical activation of H_3PO_4, *Ukrainian Food Journal*, 6(1), pp. 103–116.

10. Kuzmin O., Shendrik T. (2016), Prospective assessment of the use of the carbonized wood waste of food industry for the production of activated carbon. *Food Science for Well–being (CEFood 2016) : 8th Central European Congress on Food 2016, 23–26 May 2016, Kyiv, NUFT,* p. 109.
11. Sait Yorgun, Derya Yildiz (2015), Preparation and characterization of activated carbons from Paulownia wood by chemical activation with H_3PO_4, *Journal of the Taiwan Institute of Chemical Engineers*, 53, pp. 122–131.
12. Miroslaw Kwiatkowski, Dimitrios Kalderis, Evan Diamadopoulos (2017), Numerical analysis of the influence of the impregnation ratio on the microporous structure formation of activated carbons, prepared by chemical activation of waste biomass with phosphoric(V) acid, *Journal of Physics and Chemistry of Solids*, 105, pp. 81–85.
13. George Tzvetkov, Simona Mihaylova, Katerina Stoitchkova, Peter Tzvetkov, Tony Spassov (2016), Mechanochemical and chemical activation of lignocellulosic material to prepare powdered activated carbons for adsorption applications, *Powder Technology*, 299, pp. 41–50.
14. G. Dobele, T. Dizhbite, M.V. Gil, A. Volperts, T.A. Centeno (2012), Production of nanoporous carbons from wood processing wastes and their use in supercapacitors and CO_2 capture, *Biomass and Bioenergy*, 46, pp. 145–154.
15. Jiaojiao Kong, Qinyan Yue, Lihui Huang, Yuan Gao, Yuanyuan Sun, Baoyu Gao, Qian Li, Yan Wang (2013), Preparation, characterization and evaluation of adsorptive properties of leather waste based activated carbon via physical and chemical activation, *Chemical Engineering Journal*, 221, pp. 62–71.
16. Arvind Kumar, Hara Mohan Jena (2016), Preparation and characterization of high surface area activated carbon from Fox nut (Euryale ferox) shell by chemical activation with H_3PO_4, *Results in Physics*, 6, pp. 651–658.
17. Juan Matos, Carol Nahas, Laura Rojas, Maibelin Rosales (2011), Synthesis and characterization of activated carbon from sawdust of Algarroba wood. 1. Physical activation and pyrolysis, *Journal of Hazardous Materials*, 196, pp. 360–369.
18. Akshay Jain, Rajasekhar Balasubramanian, M.P. Srinivasan (2016), Hydrothermal conversion of biomass waste to activated carbon with high porosity, *Chemical Engineering Journal*, 283, pp. 789–805.
19. Miroslaw Kwiatkowski, Vanessa Fierro, Alain Celzard (2017), Numerical studies of the effects of process conditions on the development of the porous structure of adsorbents prepared by chemical activation of lignin with alkali hydroxides, *Journal of Colloid and Interface Science*, 486, pp. 277–286.
20. Hiroyuki Wakizaka, Hajime Miyake, Yutaka Kawahara (2016), Utilization of beer lees waste for the production of activated carbons: The influence of protein fractions on the activation reaction and surface properties, *Sustainable Materials and Technologies*, 8, pp. 1–4.
21. Piotr Nowicki, Justyna Kazmierczak, Robert Pietrzak (2015), Comparison of physicochemical and sorption properties of activated carbons prepared by physical and chemical activation of cherry stones, *Powder Technology*, 269, pp. 312–319.
22. Emine Yagmur, Meryem Ozmak, Zeki Aktas (2008), A novel method for production of activated carbon from waste tea by chemical activation with microwave energy, *Fuel*, 87 (15–16), pp. 3278–3285.
23. Ould-Idriss A., Stitou M., Cuerda-Correa E.M., Fernandez-Gonzalez C., Macias-Garcia A., Alexandre-Franco M.F., Gomez-Serrano V. (2011), Preparation of activated carbons from olive-tree wood revisited. I. Chemical activation with H_3PO_4, *Fuel Processing Technology*, 92 (2), pp. 261–265.

24. Felix A. Lopez, Teresa A. Centeno, Irene Garcia-Diaz, Francisco J. Alguacil (2013), Textural and fuel characteristics of the chars produced by the pyrolysis of waste wood, and the properties of activated carbons prepared from them, *Journal of Analytical and Applied Pyrolysis*, 104, pp. 551–558.
25. Geetha Selvaraju, Nor Kartini Abu Bakar (2017), Production of a new industrially viable green-activated carbon from Artocarpus integer fruit processing waste and evaluation of its chemical, morphological and adsorption properties, *Journal of Cleaner Production*, 141, pp. 989–999.
26. Tahira Mahmood, Rahmat Ali, Abdul Naeem, Muhammad Hamayun, Madeeha Aslam (2017), Potential of used Camellia sinensis leaves as precursor for activated carbon preparation by chemical activation with H_3PO_4; optimization using response surface methodology, *Process Safety and Environmental Protection*, 109, pp. 548–563.
27. Kucherenko V.A., Shendrik T.G., Tamarkina Yu.V., Mysyk R.D. (2010), Nanoporosity development in the thermal – shock KOH activation of brown coal, *Carbon*, 48, pp. 4556–4558.
28. Lillo-Ródenas M.A., Marco-Lozar J.P., Cazorla-Amorós D., Linares-Solano A. (2007), Activated carbons prepared by pyrolysis of mixtures of carbon precursor/alkaline hydroxide, *J. Anal. Appl. Pyrolysis*, 80(1), pp. 166–174.
29. Shendrik T.G., Simonova V.V., Kucherenko V.A., Paschenko L.V., Khabarova T.V. (2003), Adsorption properties of activated carbon from lignin, *Solid Fuel Chemistry*, 41 (1), pp. 39–44.
30. Zubkova V. (2011), Study on relation of solvent extractable material and resistivity of pyrolysed coal, *Journal of Analytical and Applied Pyrolysis*, 92, pp. 50–58.
31. Brunauer S., Emmett P.H., Teller E. (1938), Adsorption of gases in multimolecular layers, *J. Am. Chem. Soc.*, 60(2), pp. 309–319.
32. Barret E.P., Joyner L.C., Halenda P.P. (1951), The determination of pore volume and area distributions in porous substances. Computations from nitrogen isotherms, *J. Am. Chem. Soc.*, 73 (1), pp. 373–380.
33. Tramer A., Kosewska M., Wróbelska K., Winnicka G. (2006), Wpływ dodatku emulsji smołowo-wodnej na zmianę budowy warstwy plastycznej węgla w procesie pirolizy, *Karbo*, 4, pp. 195–205.
34. Xiang-Qian Zhang, Wen-Cui Li, An-Hui Lu (2015), Designed porous carbon materials for efficient CO_2 adsorption and separation, *New Carbon Materials*, 30(6), pp. 481–501.
35. Ingo Burgert, Tobias Keplinger, Etienne Cabane, Vivian Merk, Markus Rüggeberg (2016), Chapter 13 – Biomaterial Wood: Wood–Based and Bioinspired Materials, *Secondary Xylem Biology*, 2016, pp. 259–281.
36. López-Garzón F.J., Fernandez-Morales I., Moreno-Castilla C., Domingo-García M. (1999), Carbon materials as adsorbents for vapour pollutants, *Studies in Surface Science and Catalysis*, 120(B), pp. 397–433.
37. Menéndez-Díaz J.A., Martín-Gullón I. (2006), Chapter 1. Types of carbon adsorbents and their production, *Interface Science and Technology*, 7, 2006, pp. 1–47.